applied sciences

MDPI

Brief Report

A Sustainable Electrochemical-Based Solution for Removing Acetamiprid from Water

Alana Maria Nunes de Morais [1], Danyelle Medeiros Araújo [2,3], Inalmar Dantas Barbosa Segundo [3], Elisama Vieira dos Santos [2,3], Suely Souza Leal de Castro [1], Carlos A. Martínez-Huitle [2,3,*] and Janete Jane Fernandes Alves [1]

[1] Faculty of Exact and Natural Sciences, State University of Rio Grande do Norte, Campus Central, Mossoro 59625-620, RN, Brazil; alanaamorais@gmail.com (A.M.N.d.M.); suelycastro@uern.br (S.S.L.d.C.)
[2] National Institute for Alternative Technologies of Detection, Toxicological Evaluation and Removal of Micropollutants and Radioactives (INCT-DATREM), Institute of Chemistry, Universidade Estadual Paulista, P.O. Box 355, Araraquara 14800-900, SP, Brazil; elisama_quimica@yahoo.com.br (E.V.d.S.)
[3] Renewable Energies and Environmental Sustainability Research Group, Institute of Chemistry, Federal University of Rio Grande do Norte, Campus Universitário, Av. Salgado Filho 3000, Lagoa Nova, Natal 59078-970, RN, Brazil; idbsegundo@gmail.com
* Correspondence: carlosmh@quimica.ufr.br or carlos.alberto.mh@ufrn.br

Abstract: Pesticides are used worldwide in agriculture to prevent insects and other pests that attack plants and their derivatives. Acetamiprid (ACT) is a type of insecticide belonging to the chemical group of neonicotinoids, which are widely used in agricultural planting to replace organophosphates. Therefore, in this work, the performance of the electrochemical oxidation (EO) process as an alternative solution to eliminate pesticides in water was evaluated. A dimensionally stable anode (DSA, TiO_2-RuO_2-IrO_2) and boron-doped diamond (BDD) were tested as anodes for degrading ACT (30 and 300 mg L^{-1}) by using different applied current densities (*j*): 30, 60, 90, and 120 mA cm^{-2}. The degradation process was monitored by using ACT decay, spectrophotometric analysis, and chemical oxygen demand. The results clearly showed that ACT (30 mg L^{-1}) was only eliminated from water at the DSA electrode when 90 mA cm^{-2} was applied, reaching higher removal efficiencies after 180 min of electrolysis. Conversely, ACT was quickly removed at all applied current densities used, at the same concentration. On the other hand, when the ACT concentration was increased (300 mg L^{-1}), 71.4% of the COD removal was reached by applying 90 mA cm^{-2} using BDD, while no significant improvements were achieved at the DSA electrode when a higher concentration of ACT was electrochemically treated.

Keywords: pesticide; acetamiprid; electrochemical oxidation; wastewater treatment

Citation: Nunes de Morais, A.M.; Medeiros Araújo, D.; Barbosa Segundo, I.D.; Vieira dos Santos, E.; Leal de Castro, S.S.; Martínez-Huitle, C.A.; Fernandes Alves, J.J. A Sustainable Electrochemical-Based Solution for Removing Acetamiprid from Water. *Appl. Sci.* **2023**, *13*, 10963. https://doi.org/10.3390/app131910963

Academic Editor: Juan García Rodríguez

Received: 20 August 2023
Revised: 17 September 2023
Accepted: 21 September 2023
Published: 4 October 2023

1. Introduction

Pesticides are used worldwide in agriculture to eliminate and/or prevent insects present in plants and their derivatives, thus ensuring the production of sufficient food to meet the alimentary needs of humans [1]. However, the continuous release of these organic substances has been causing serious problems for the environment, including the aquatic environment [2,3]. Among all organic pollutants found in wastewater, pesticides deserve attention due to their excessive use and because they become very toxic over time, being considered recalcitrant compounds. Therefore, the elimination of these substances from water has become a challenge [4,5]. Within this framework, the incessant search for treatment technologies was initiated to eliminate so-called persistent organic pollutants (POPs), including pesticides. Conventional treatments such as biological and physical-chemical processes are not sufficient to remove these substances from wastewater at levels of μg L^{-1}–ng L^{-1}, since these processes together with other environmental factors favor the

accumulation of such pollutants in lakes, rivers, oceans, and even in drinking water [6]. Then, there is a need to develop advanced treatment technologies to effectively eliminate potentially toxic compounds that can not be removed by conventional processes.

In recent years, electrochemical advanced oxidation processes (EAOPs) have received great attention as an alternative technology for removing organic pollutants from synthetic [7–9] and/or real water matrices in multistage [9,10] or single-stage systems [9,11]. EAOPs are treatment methods that are considered promising for the environment since organic compounds can be destroyed until mineralization after the attack of the hydroxyl radical generated in situ (•OH). This oxidizing species has a high standard redox potential ($E° = 2.80$ V/SHE), and this characteristic guarantees its ability to oxidize organic pollutants [12–14]. Diamond electrodes are considered the best non-active anodes in EO due to their great effectiveness in mineralizing different organic pollutants in wastewater treatment by free heterogeneous •OH (an indirect oxidation approach where electrochemical mineralization is promoted), whereas mixed-metal oxides (MMO) or dimensionally stable anodes (DSA) are considered active anodes [15–18]. Active anodes favor electrochemical conversion by direct interaction (chemisorption) between organic molecules (reactants or products) at the surface, and the hydroxyl radicals are also stabilized at their surface, forming higher oxidation states [18].

Therefore, this work aims to evaluate the degradation of a commercial formulation containing ACT by using DSA and BDD anodes with different *j* and initial concentrations of the target pollutant, monitoring ACT elimination by spectrophotometric and COD analysis. The development of technologies and smart water solutions to reach Sustainable Development Goal 6 (SDG6) by using EAOPs represents a substantial opportunity to guarantee sustainability and increase competence in water management (to treat and distribute water for human use) [19]. Then, efficient SDG6-based electrochemical technologies can be established for eliminating ACT in or from real water samples as a clear benefit for our society, offering a coherent vision for the future [19].

2. Materials and Methods

2.1. Reagents and Solutions

The commercial ACT insecticide used was from STK (N-[(6-chloropyridin-3-yl)methyl]-N-cyano-N-methylethanimidamide; $C_{10}H_{11}ClN_4$, 20% purity, Stockton Group), and the solutions were prepared using distilled water at concentrations of 30 and 300 mg L^{-1}. Sodium sulfate (Na_2SO_4) at 0.5 mol L^{-1} was used as a supporting electrolyte to increase the electrical conductivity of the medium and was purchased from Fluka.

2.2. Electrolytic System and Analytical Procedures

Two anodes were used in the present study and were provided by De Nora (Brazil, TiO_2-RuO_2-IrO_2) and the Electrochemistry and Environmental Engineering laboratory at the Universidad de Castilla-La Mancha (Spain, BDD). A titanium plate was used as the cathode. Both electrodes had a geometrical area of about 18 cm^2. The ACT electrochemical oxidation experiments (500 mL of solution), under magnetic stirring conditions, were carried out in a single-sharing electrochemical cell, applying different *j* (30, 60, 90, and 120 mA cm^{-2}) with a power supply (model MLP-3303, 3A/5V, Minipa) in a supporting electrolyte of 0.5 mol L^{-1} Na_2SO_4. During the electrolysis, samples of 10 mL were collected to perform a complete wavelength scan from 200 to 800 nm (Varian Cary 50 Conc UV-Visible Spectrophotometer) and COD analysis. The detection wavelength of ACT was 245 nm, which is the peak value reported in the literature by Padervand et al. (2020) when working with the degradation of standard ACT. COD was performed using a set of HANNA kits' reagent bottles following the Environmental Protection Agency (EPA) method for determining COD in the medium range (0–1500 ppm, Ref. HI93754B-25) [20]. Three measurements were taken, and the average value with a standard deviation of <3% was recorded. pH conditions were monitored using a pH meter (TECNAL, model PG2000).

Additionally, water quality was assessed according to the international standard DIN EN ISO 7887 (2012-04) as reported elsewhere, where the examination and determination of color is conducted. The solution coloration was analyzed by estimating the parameter DFZ (Deutsche Farb Zah) (m^{-1}) from the solution. The absorbance at characteristic wavelengths (λ = 436 nm, λ = 525 nm, and λ = 620 nm) was taken from the UV-vis spectrum between 200 and 800 nm. DFZ estimation allows complex case evaluation of effluent coloration by considering these characteristic wavelengths, and then DFZy was calculated according to equation (1) following the method DIN EN 7884:2012 [21].

$$DFZ_y = 100 \times (E_y/d) \quad (1)$$

where Ey is the absorbance at a y wavelength, and d is the cell path length in cm.

3. Results

3.1. Linear Polarization Curves

Figure 1 compares the linear polarization curves of the DSA and BDD electrodes obtained at a lower concentration of commercial ACT (30 mg L^{-1}) using 0.5 M Na_2SO_4 as the supporting electrolyte with a scan rate of 100 mV s^{-1}. The DSA anodic polarization curve shows that the oxygen evolution reaction (o.e.r.) starts at a potential close to +1.2 V vs. Ag/AgCl, confirming the active anode behavior towards oxygen evolution [22–26]. Conversely, the o.e.r. is attained at about +1.7 V vs. Ag/AgCl at the BDD anode according to the polarization curve (Figure 1), presenting a higher oxygen potential than that achieved at the DSA anode. This is an expected result since non-active anodes have higher oxygen potentials than active anodes [27]. Thus, the BDD anode has a higher energy efficiency during the degradation of organic compounds in solution when compared to the DSA electrode [26].

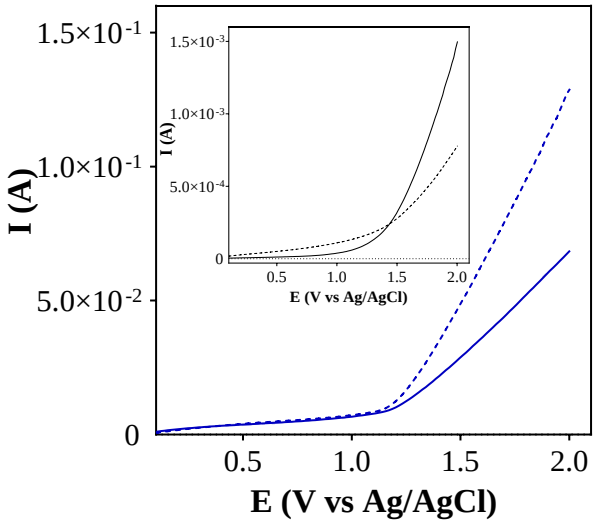

Figure 1. Linear polarization curves of the DSA (blue lines) and BDD (black lines) electrodes in a solution of 0.5 M of Na_2SO_4, without (bold line) or with (dashed line) 30 mg L^{-1} of commercial ACT in solution. Scan rate, 100 mV s^{-1} at 25 °C.

On the other hand, a different behavior was observed when a well-known concentration of ACT was added to the solution (Figure 1). For example, when 30 mg L^{-1} of ACT was added to the supporting electrolyte in the electrochemical cell (dashed lines in Figure 1), a significant increase in the current response was observed at the DSA electrode, shifting the o.e.r. to lower potential values (+1.01 V). This behavior suggests that a direct electron transfer mechanism between the ACT molecule and the TiO_2-RuO_2-IrO_2 electrode occurs, revealing the possibility of partial organic molecule adsorption on its active sites [26,28]. Conversely, at the concentration of ACT under study, the voltametric profile registered at

the BDD anode in 0.5 M of Na_2SO_4 (dashed line in the inset of Figure 1) displays a distinct behavior from that observed at the TiO_2-RuO_2-IrO_2 electrode. In this case, a large decrease in current is observed in the region of the o.e.r. as a result of the efficient degradation of ACT in solution by the hydroxyl radicals produced by water discharge and/or as a partial deactivation of the diamond surface [9,28]. Then, a set of experiments at the batch electrochemical cell were carried out to better understand the degradation efficiency and mechanism attained.

3.2. Influence of Different j on the EO of ACT

The study of the effect of *j* on ACT removal at the TiO_2-RuO_2-IrO_2 electrode as a function of electrolysis time was accompanied by the decay of the absorption bands (Figure 2a 30, Figure 2b 60, Figure2c 90, and Figure 2d 120 mA cm^{-2}). The results indicated that the characteristic ACT absorption band at 245 nm decayed, until it disappeared, as a function of electrolysis time and *j*. This decay is associated with the increase in the *j* [28]. When 30 and 60 mA cm^{-2} were applied (Figure 2a,b), intense absorption bands were still observed up to 120 min of electrolysis, indicating that a low *j* did not significantly influence the insecticide degradation at the beginning of the process. However, when an increase in *j* (Figure 2c,d) is applied, intense absorption bands were observed only up to 60 and 30 min of electrolysis, when 90 and 120 mA cm^{-2} were applied, respectively. This behavior confirms that an increase in the *j* increased the ACT removal rate [8,21,28], as is also observed in Figure 3, which shows a comparison of the influence of *j* on the EO of ACT using normalized maximum absorption as a function of electrolysis time. At 90 and 120 mA cm^{-2}, more significant removal rates were reached with short electrolysis times, while at lower j (30 and 60 mA cm^{-2}), the decline in absorbance associated with the ACT characteristic band exhibited a slower rate of removal. Another feature that should be commented on is that at higher *j* (90 and 120 mA cm^{-2}), the formation of a new absorption band at 275 nm is observed as a consequence of the formation of by-products during ACT degradation [9,29].

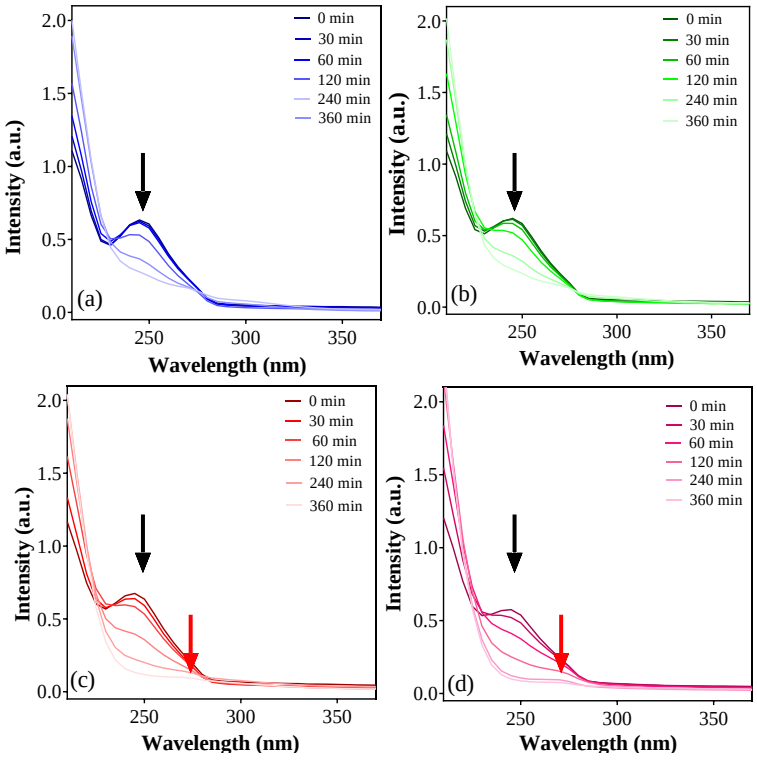

Figure 2. Absorption spectra as a function of electrolysis time during the EO of 30 mg L^{-1} of ACT at DSA by applying different *j*: (**a**) 30, (**b**) 60, (**c**) 90, and (**d**) 120 mA cm^{-2}. Operating conditions: 0.5 M Na_2SO_4 and 25 °C. Black and red arrows in the UV-vis spectra (a-d) indicate the bands related to ACT (245 nm) and to a by-product (275 nm), respectively.

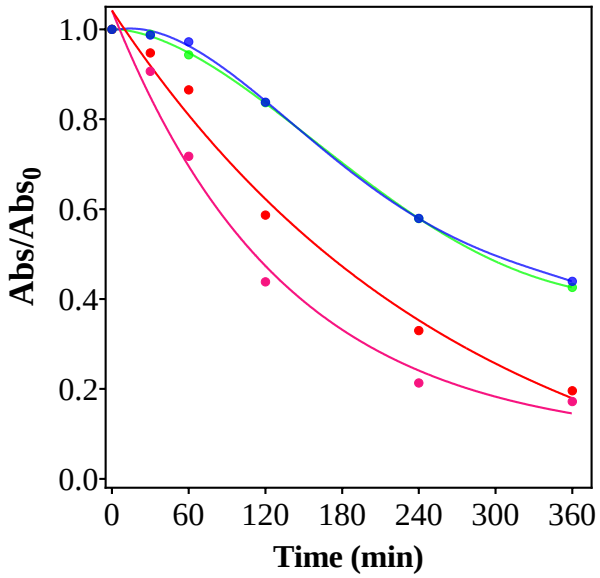

Figure 3. Comparison of the influence of *j* on the EO of 30 mg L^{-1} of ACT using DSA anode as a function of electrolysis time.

Considered an active anode, the degradation of ACT with Ti/TiO_2-RuO2-IrO_2 occurs mainly via higher oxides generated on its surface [28], especially at higher *j* (Equations (2) and (3)). This anode also promotes o.e.r. (Equation (4)), which occurs in parallel with the degradation of ACT, becoming an undesired reaction at higher *j* and consequently making the degradation process more difficult [30–32]. This behavior explains the lack of complete removal of ACT at different *j*, proving that at a determined point, the o.e.r. takes place over the hydroxyl radicals' performance. These assertions are in agreement with the behaviors observed at the polarization curves in Figure 2, where a direct oxidation mechanism was suggested at the DSA electrode, which was influenced by the o.e.r. [32–35].

$$MO_x(^{\bullet}OH) \rightarrow MO_{x+1} + H^+ + e^- \quad (2)$$

$$MO_{x+1} + R \rightarrow RO + MO_x \quad (3)$$

$$MO_{x+1} \rightarrow MO_x + \tfrac{1}{2}\, O_2 \quad (4)$$

The influence of the *j* on the degradation of ACT with the BDD anode is shown in Figure 4. These results indicate that the degradation of ACT occurred in 30 min of electrolysis. Comparing the absorption spectra obtained with DSA electrolysis with those achieved with BDD, it is possible to observe that, with the former, the characteristic ACT absorption band was gradually reduced, whereas it quickly disappears at all *j* values after 5 min of electrolysis with the latter. Unlike DSA, the BDD anode is considered a non-active electrode, therefore, organic compounds are quickly oxidized by free hydroxyl radicals produced at the diamond surface [15–17,23,35]. This follows the results observed in Figure 2, as the oxygen evolution potential of the non-active anodes has a potential greater than that presented by active electrodes (see Figure 2). Thus, the evolution of oxygen is slower at this type of electrode, and consequently, the production of hydroxyl radicals is significantly favored, which accelerates the oxidation process [17,18,23,35]. Nevertheless, it is important to remark that the use of BDD as an anode and the significative concentration of sulfate ions in solution, due to the electrolyte, promotes the electrosynthesis of sulfate-based oxidants (ion sulfate radical (Equation (5)) and persulfate (Equations (6) and (7)) [36]) that participate in the indirect oxidation of the organic compounds [14,37–40].

$$SO_4^{2-} \rightarrow SO_4^{\bullet -} + e^- \quad (5)$$

$$SO_4^{\bullet -} + SO_4^{2-} \rightarrow S_2O_8^{2-} \quad (6)$$

$$S_2O_8^{2-} + e^- \rightarrow SO_4^{\bullet -} + SO_4^{2-} \quad (7)$$

The participation of sulfate-based oxidants plays a key role in the efficient degradation of ACT at all *j* values because no other absorption bands appear in the final phase of the electrochemical treatment (Figure 4). Then, no absorptive by-products were generated from BDD electrolysis, contrary to the behavior at the Ti/TiO_2-RuO_2-IrO_2 anode (see Figure 3).

From an environmental point of view, some physical–chemical parameters were measured before and after the EO of synthetic effluents (Table 1). DFZ values (Equation (1)) were also estimated [21] to establish the wastewater quality of the real effluent (Table 1), and the result showed that the treated effluent could be reused (e.g., for irrigation or washing) when the BDD anode was used. Nevertheless, the data obtained at the DSA electrode demonstrated that the treatment could still be improved.

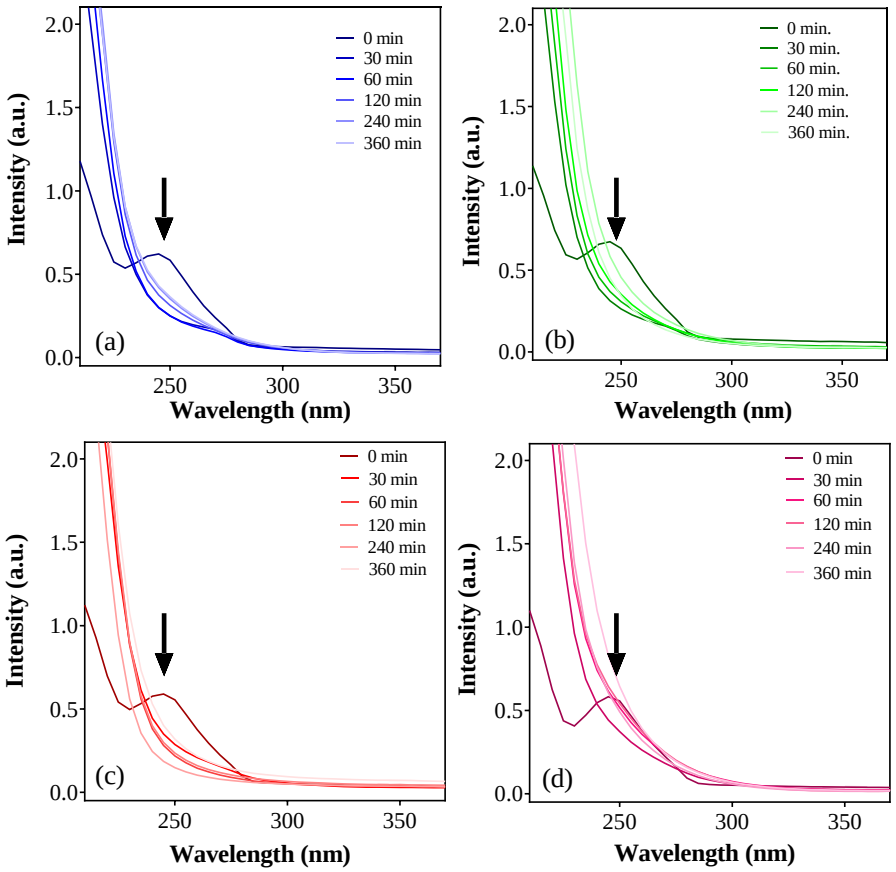

Figure 4. Absorption spectra as a function of electrolysis time during the EO of 30 mg L^{-1} of ACT at BDD by applying different *j*: (**a**) 30, (**b**) 60, (**c**) 90, and (**d**) 120 mA cm^{-2}. Operating conditions: 0.5 M Na_2SO_4 and 25 °C. Black arrows in the UV-vis spectra (a-d) indicate the bands related to ACT (245 nm).

Table 1. Physicochemical characterization of effluent, before and after different treatment.

Parameters		Synthetic Effluent	After Treatment	
			DSA	BDD
Color (DFZ units, m^{-1})	436 nm	98.4	32.6	6.1
	525 nm	89.2	28.1	3.4
	620 nm	64.1	15.7	3.7
Conductivity (mS cm^{-1})		20.8	19.4	11.5
Salinity (psu)		18.5	17.54	13.85
pH		7.74	6.5	5.9

Turbidity (NTU)	23	43	21
$COD_{30\ mA\ cm^{-2}}$ (mg L^{-1})	32.5	25,6	15.7
$COD_{60\ mA\ cm^{-2}}$ (mg L^{-1})		18.5	10.2
$COD_{90\ mA\ cm^{-2}}$ (mg L^{-1})		16.8	7.4
$COD_{120\ mA\ cm^{-2}}$ (mg L^{-1})		15.8	6.2

Thus, these results demonstrated that higher decontamination of the effluent was achieved when the degradation pathway was guided by hydroxyl radicals and sulfate-based oxidizing species in a sulfate-mediated solution [9,21], but the organic matter removal should be also determined. Therefore, the determination of COD was carried out at the end of the electrolysis using both materials. Analyzing the data obtained at the end of electrolysis using both materials (Table 1), it is evident that the EO process favored the elimination of organic matter dissolved (ACT and by-products) in the synthetic effluent. However, high oxidation efficacy was demonstrated by the BDD anode. In the case of salinity and conductivity, these values slightly decreased with both EO-based treatments due to the use of the electrolyte, and it was combined in different ways. When the DSA electrode was used, no significant changes were observed; in contrast to the significant decrease achieved at the BDD anode because the sulfate ions were electrochemically converted to persulfate, causing a significant decrease in conductivity and salinity. Turbidity was initially observed due to the preparation of the ACT solution; however, it disappeared after the electrolysis, and the values measured after the treatment are a consequence of the faint color.

3.3. Effect of the Initial ACT Concentration on Its Electrochemical Elimination

From the investigation of the EO of ACT at different *j* with lower concentrations (30 mg L^{-1}), it can be observed that, in general, by applying higher *j* values, the best behaviors at both anodes were obtained. Given the above, a set of experiments was performed by applying 90 mA cm^{-2} to limit higher energy consumption and avoid o.e.r. as an undesired reaction. At this point, the ACT concentration increased, and the synthetic effluent was electrolyzed with the Ti/TiO_2-RuO_2-IrO_2 and BDD anodes.

Figure 5 shows the absorbance spectra for removing ACT at a concentration of 300 mg L^{-1} by applying 90 mA cm^{-2} as a function of electrolysis time using the DSA and BDD electrodes. As illustrated in Figure 5, on the one hand, the absorption band at 245 nm decreases at both EO-based processes, but it quickly decays at the BDD anode rather than the Ti/TiO_2-RuO_2-IrO_2 anode. On the other hand, the increase in the initial ACT concentration promotes the generation of the by-product at both anodes, and a new absorptive band appears at 275 nm, as described in Figure 2, consequently requiring a greater degradation of the organic compounds present there [41].

As analyzed at the concentration of 30 mg L^{-1}, the oxidation efficacy of the BDD anode is due to the key role of the hydroxyl radicals and sulfate-based oxidizing species electrogenerated at its surface in a sulfate-mediated solution. Conversely, no persulfate production is observed at the DSA electrode, and the generation of free hydroxyl radicals is more restricted because of its active nature [9,14].

Figure 6 depicts a comparison between the DSA and BDD performance in removing ACT with EO treatment at 90 mA cm^{-2}. In this way, it is evident that after 5 min of electrolysis using the BDD anode, substantial removal is achieved, while DSA gradually eliminates ACT until 360 min.

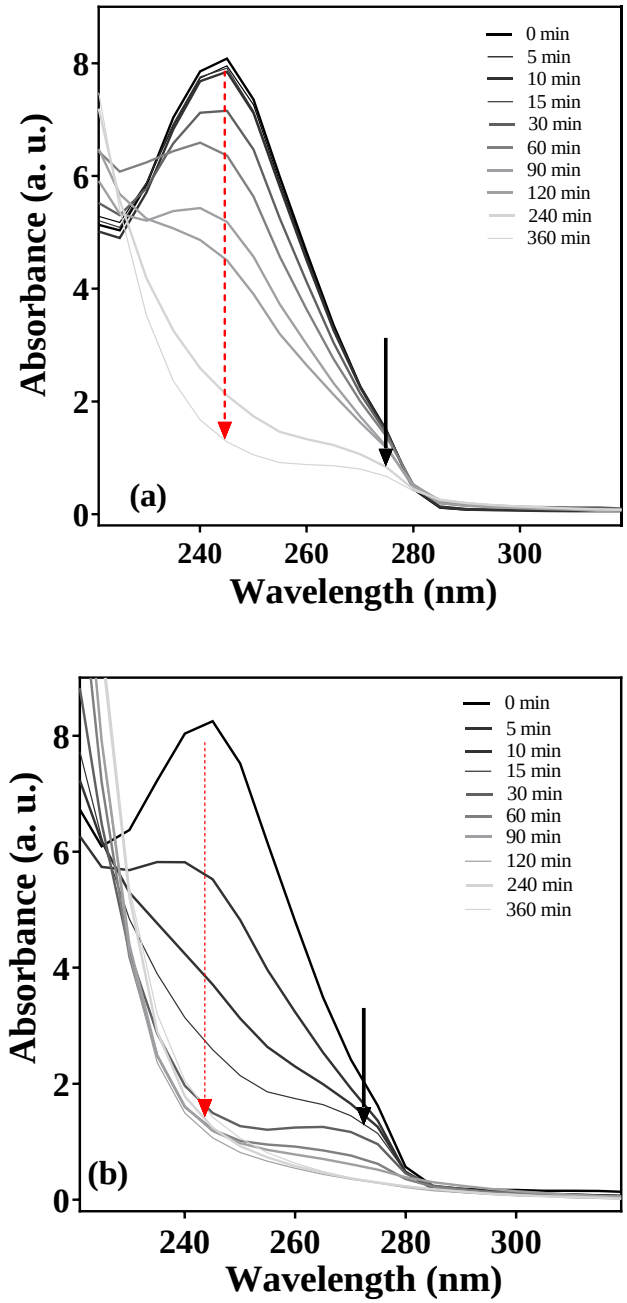

Figure 5. Absorption spectra of ACT during the EO of 300 mg L^{-1} of ACT at (**a**) DSA and (**b**) BDD electrodes, as a function of electrolysis time. Operating conditions: 90 mA cm^{-2}, 0.5 M Na_2SO_4 and 25 °C. Red and black arrows in the UV-vis spectra (a-d) indicate the bands related to ACT (245 nm) and to a by-product (275 nm), respectively.

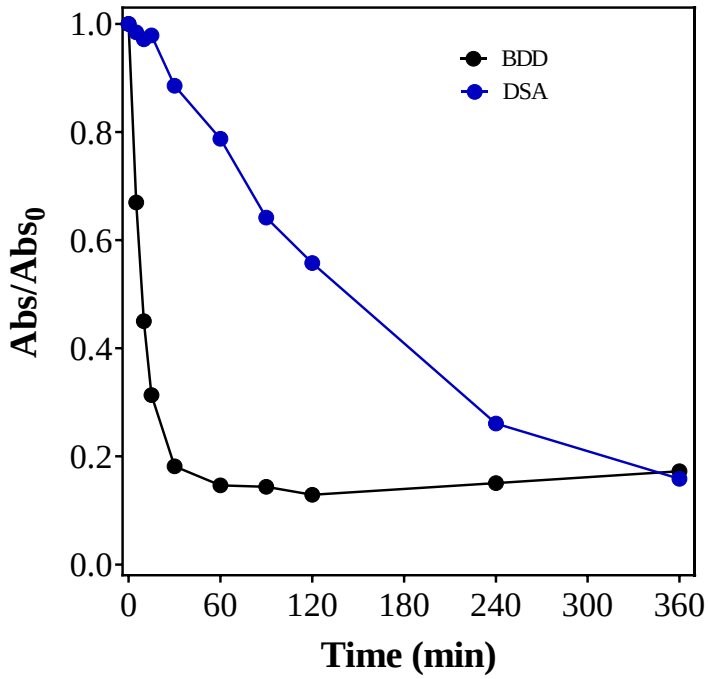

Figure 6. Comparison between BDD and DSA anodes during EO of commercial ACT (300 mg L^{-1}) solution as a function of electrolysis time. Operating conditions: 90 mA cm^{-2}, 0.5 M Na_2SO_4 and 25 °C.

3.4. COD Decay

To carry out a more evident comparative analysis, Figure 7a depicts the normalized COD decay as a function of time at 90 mA cm^{-2} in 0.5 M Na_2SO_4. It was observed that until the period of 60 min of electrolysis, COD decay using the DSA anode was only 47.5%. Meanwhile, at the BDD anode, a more efficient removal was achieved (71.4%). It is important to note that the COD value may be also associated with the generation and increase of intermediates in the treated solution [42]; then, more treatment time is needed to eliminate ACT and all the by-products generated during the EO process. For this reason, the comparison between electrocatalytic materials was performed to determine the best operating conditions for the ACT treatment, allying removal of the contaminants and the best energy efficiency (Figure 7b).

After analyzing the performance of the EO of synthetic ACT effluent by applying 90 mA cm^{-2}, the effect on the increase of the ACT concentration demonstrated that the cost of the treatment increases as a function of *j* (Figure 7b), being more significative when BDD was used as an anode [8,20,21,43]. Another feature is that it is clear that even when the BDD anode promotes better results, achieving higher COD removal efficiencies, the DSA electrode requires lower energy consumption (inset in Figure 7b). However, 60% COD removal could be achieved under the described operating conditions at the BDD anode with modest energy requirements, and a post-treatment could be applied [9].

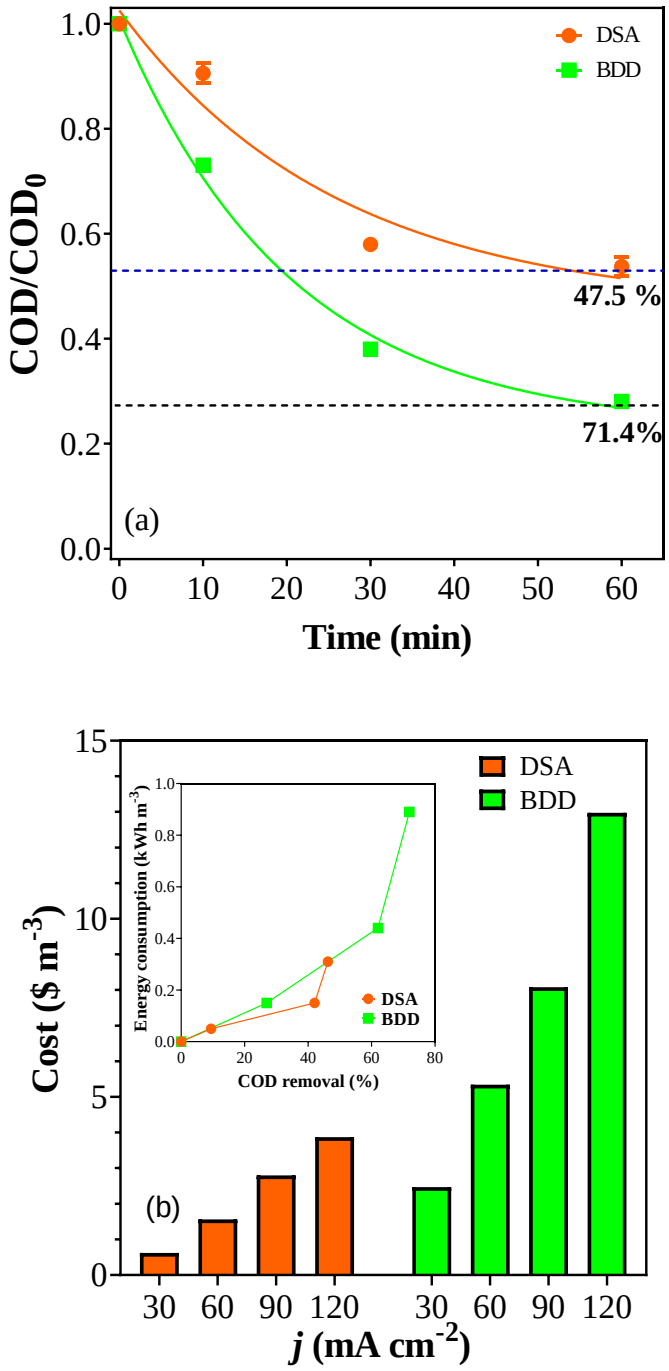

Figure 7. (**a**) COD removal as a function of electrolysis time during the EO; and (**b**) cost analysis (USD 0.15 per kWh m^{-3}) depending on the used *j* and energy consumption by COD removal (inset). Operating conditions: 300 mg L^{-1} of ACT by applying 90 mA cm^{-2}, 0.5 M Na_2SO_4, and 25 °C.

Based on the existing literature, hypothetical degradation pathways of ACT during the EO process were proposed from the 19 degradation intermediates identified by Yao and co-workers [44] when a Yb-doped PbO_2 electrode was used in 0.05 mol L^{-1} Na_2SO_4 solution. The three degradation pathways proposed (demethylation, decyanation, and hydroxylation) were identified as I, II, and III sub-routes according to the different initial attacking ACT positions on three active functional groups by hydroxyl radicals (Figure 8) [44]. Sub-route I was divided into I-1 and I-2 degradation pathways that correspond to

dechlorination and demethylation starting reactions, respectively, with successive steps (Figure 8).

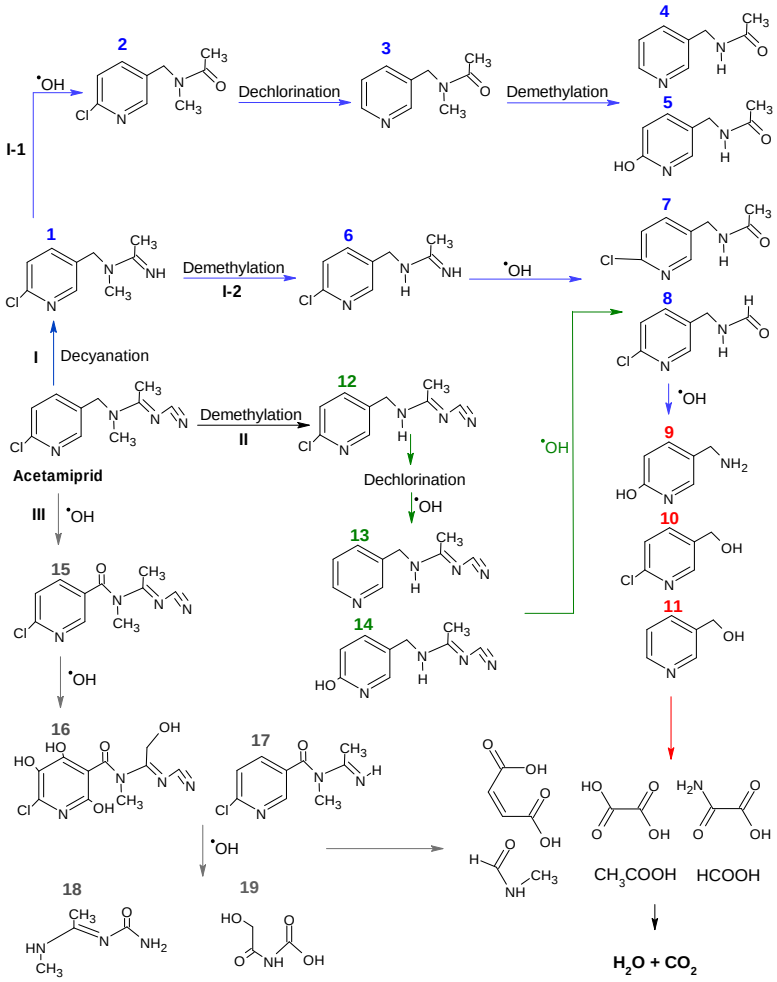

Figure 8. Proposed ACT degradation mechanisms [44]. The color arrows indicate the different degradation mechanisms.

However, Yao and co-workers [44] have considered in two routes (I-1 and III) the attack of the hydroxyl radicals (in sub-route I-1, only after a decyanation, but it could be simultaneously attained with hydroxyl radical reaction) as a starting degradation step (a radical reaction). Then, similar degradation pathways can be hypothesized at the BDD anode in this work; nevertheless, three additional degradation reactions have been not considered, such as an auto-catalytic reaction mediated by Cl^-, which is released by chlorinated-organic compounds after hydroxyl radicals attack [45], the non-radical reactions promoted by persulfate, and the radical reactions favored by ion sulfate radicals [14]. Then, further experiments should be performed to identify the intermediates and, subsequently, determine the possible degradation mechanisms as well as the use of renewable energies to decrease the remediation cost and/or the production of high value-added products like aromatic compounds, carboxylic acids, and green hydrogen [46,47].

4. Conclusions

In this study, we investigated the electrocatalytic activity of Ti/TiO_2-RuO_2-IrO_2 (active anode) and BDD (non-active anode) in the EO of ACT insecticide in a synthetic effluent. In general, the two electrodes presented good oxidative performance, whereas BDD showed better results in degradation time and COD removal. These results can be explained by the fact that non-active anodes have higher oxygen potentials than active

anodes, and this characteristic causes the evolution of oxygen to start at higher potentials, and consequently, produce electrochemically more hydroxyl radicals than that generated at the DSA electrode.

On the one hand, when working with a concentration of 30 mg L^{-1}, it was observed that when the removal time was compared, the BDD and DSA anodes presented different degradation performance times of about 30 and 120 min, respectively, by applying lower *j* (30 mA cm^{-2}) and having the BDD electrode benefit in degradation time. However, when *j* was increased, the degradation time gradually decreased at both anodes, with BDD being superior to the DSA anode. On the other hand, when the insecticide concentration was 300 mg L^{-1}, and *j* was 90 mA cm^{-2}, COD removal efficiencies of about 71.4% and 47.5% were achieved, respectively, at the BDD and DSA anodes. Within this framework, at lower COD, ACT removal depends on the mass-transport conditions [44] and the nature of the anode material. However, no limitations were observed at higher ACT concentrations, removing more efficiently the pollutant from synthetic effluent. However, the use of BDD implies high treatment costs, which can be further investigated if the treatment strategy demonstrated here is pursued for actual implementation.

Author Contributions: Conceptualization, E.V.d.S., C.A.M.-H., S.S.L.d.C. and J.J.F.A.; methodology, A.M.N.d.M. and D.M.A.; formal analysis, D.M.A. and A.M.N.d.M.; resources, I.D.B.S., A.M.N.d.M., D.M.A. and C.A.M.-H.; data curation, E.V.d.S., C.A.M.-H., I.D.B.S., D.M.A. and S.S.L.d.C.; writing—original draft preparation, A.M.N.d.M. and I.D.B.S.; writing—review and editing, I.D.B.S., E.V.d.S., C.A.M.-H., D.M.A. and J.J.F.A.; funding acquisition, S.S.L.d.C., I.D.B.S., E.V.d.S., C.A.M.-H. and D.M.A. All authors have read and agreed to the published version of the manuscript.

Funding: This research was funded by Conselho Nacional de Desenvolvimento Científico e Tecnológico (Brazil), grant number 152760/2022-9 and 116925/2022-1, and Fundação de Amparo à Pesquisa do Estado de São Paulo (Brazil), grant numbers 2014/50945-4 and 2019/13113-4.

Institutional Review Board Statement: Not applicable.

Informed Consent Statement: Not applicable.

Data Availability Statement: Data available on request due to restrictions eg., privacy or ethical.

Acknowledgments: Financial supports from the Conselho Nacional de Desenvolvimento Científico e Tecnológico (CNPq–152760/2022-9 and 116925/2022-1) and Fundação de Amparo à Pesquisa do Estado de São Paulo (Brazil) (FAPESP 2014/50945-4 and 2019/13113-4) are gratefully acknowledged.

Conflicts of Interest: The authors declare no conflicts of interest.

References

1. Yang, Y.; Xia, Y.; Wei, F.; Zhang, L.; Yao, Y. Electrochemical Oxidation of the Pesticide Nitenpyram Using a Gd-PbO_2 Anode: Operation Parameter Optimization and Degradation Mechanism. *J. Chem. Technol. Biotechnol.* **2020**, *95*, 2120–2128. https://doi.org/10.1002/jctb.6397.
2. Brillas, E. A Review on the Photoelectro-Fenton Process as Efficient Electrochemical Advanced Oxidation for Wastewater Remediation. Treatment with UV Light, Sunlight, and Coupling with Conventional and Other Photo-Assisted Advanced Technologies. *Chemosphere* **2020**, *250*, 126198. https://doi.org/10.1016/j.chemosphere.2020.126198.
3. Barbosa Segundo, I.D.; Martins, R.J.E.; Boaventura, R.A.R.; Silva, T.F.C.V.; Moreira, F.C.; Vilar, V.J.P. Finding a Suitable Treatment Solution for a Leachate from a Non-Hazardous Industrial Solid Waste Landfill. *J. Environ. Chem. Eng.* **2021**, *9*, 105168. https://doi.org/10.1016/J.JECE.2021.105168.
4. Rezgui, S.; Amrane, A.; Fourcade, F.; Assadi, A.; Monser, L.; Adhoum, N. Electro-Fenton Catalyzed with Magnetic Chitosan Beads for the Removal of Chlordimeform Insecticide. *Appl. Catal. B* **2018**, *226*, 346–359. https://doi.org/10.1016/j.apcatb.2017.12.061.
5. Sharma, A.; Kumar, V.; Shahzad, B.; Tanveer, M.; Sidhu, G.P.S.; Handa, N.; Kohli, S.K.; Yadav, P.; Bali, A.S.; Parihar, R.D.; et al. Worldwide Pesticide Usage and Its Impacts on Ecosystem. *SN Appl. Sci.* **2019**, *1*, 1446.
6. Martínez-Huitle, C.A.; Brillas, E. Decontamination of Wastewaters Containing Synthetic Organic Dyes by Electrochemical Methods: A General Review. *Appl. Catal. B* **2009**, *87*, 105–145. https://doi.org/10.1016/J.APCATB.2008.09.017.

7. Vernasqui, L.G.; dos Santos, A.J.; Fortunato, G.; Kronka, M.S.; Barazorda-Ccahuana, H.L.; Fajardo, A.S.; Ferreira, N.G.; Lanza, M.R. Highly Porous Seeding-Free Boron-Doped Ultrananocrystalline Diamond Used as High-Performance Anode for Electrochemical Removal of Carbaryl from Water. *Chemosphere* **2022**, *305*, 135497. https://doi.org/10.1016/j.chemosphere.2022.135497.
8. da Silva, J.C.O.; Solano, A.M.S.; Barbosa Segundo, I.D.; dos Santos, E.V.; Martínez-Huitle, C.A.; da Silva, D.R. Achieving Sustainable Development Goal 6 Electrochemical-Based Solution for Treating Groundwater Polluted by Fuel Station. *Water* **2022**, *14*, 2911. https://doi.org/10.3390/W14182911.
9. Martínez-Huitle, C.A.; Rodrigo, M.A.; Sirés, I.; Scialdone, O. A Critical Review on Latest Innovations and Future Challenges of Electrochemical Technology for the Abatement of Organics in Water. *Appl. Catal. B* **2023**, *328*, 122430. https://doi.org/10.1016/J.APCATB.2023.122430.
10. Barbosa Segundo, I.D.; Moreira, F.C.; Silva, T.F.C.V.; Webler, A.D.; Boaventura, R.A.R.; Vilar, V.J.P. Development of a Treatment Train for the Remediation of a Hazardous Industrial Waste Landfill Leachate: A Big Challenge. *Sci. Total Environ.* **2020**, *741*, 140165. https://doi.org/10.1016/J.SCITOTENV.2020.140165.
11. Abdulgani, I.; Escalona-Durán, F.; de Araújo, D.M.; dos Santos, E.; Barbosa Segundo, I.D.; Martínez-Huitle, C.A. The Role of Saline-Related Species in the Electrochemical Treatment of Produced Water Using Ti/IrO_2-Ta_2O_5 Anode. *J. Electroanal. Chem.* **2022**, *910*, 116163. https://doi.org/10.1016/J.JELECHEM.2022.116163.
12. Nidheesh, P.; Zhou, M.; Oturan, M.A. An Overview on the Removal of Synthetic Dyes from Water by Electrochemical Advanced Oxidation Processes. *Chemosphere* **2018**, *197*, 210–227. https://doi.org/10.1016/j.chemosphere.2017.12.195.
13. Ganiyu, S.O.; Martínez-Huitle, C.A. Nature, Mechanisms and Reactivity of Electrogenerated Reactive Species at Thin-Film Boron-Doped Diamond (BDD) Electrodes During Electrochemical Wastewater Treatment. *ChemElectroChem* **2019**, *6*, 2379–2392. https://doi.org/10.1002/celc.201900159.
14. Araújo, K.C.; dos Santos, E.V.; Nidheesh, P.V.; Martínez-Huitle, C.A. Fundamentals and Advances on the Mechanisms of Electrochemical Generation of Persulfate and Sulfate Radicals in Aqueous Medium. *Curr. Opin. Chem. Eng.* **2022**, *38*, 100870. https://doi.org/10.1016/J.COCHE.2022.100870.
15. Clematis, D.; Panizza, M. Electrochemical Oxidation of Organic Pollutants in Low Conductive Solutions. *Curr. Opin. Electrochem.* **2021**, *26*, 100665. https://doi.org/10.1016/j.coelec.2020.100665.
16. Clematis, D.; Panizza, M. Application of Boron-Doped Diamond Electrodes for Electrochemical Oxidation of Real Wastewaters. *Curr. Opin. Electrochem.* **2021**, *30*, 100844. https://doi.org/10.1016/J.COELEC.2021.100844.
17. Pérez, J.; Llanos, J.; Sáez, C.; López, C.; Cañizares, P.; Rodrigo, M. Development of an innovative approach for low-impact wastewater treatment: A microfluidic flow-through electrochemical reactor. Chem. Eng. J. **2018**, *351*, 766–772. https://doi.org/10.1016/j.cej.2018.06.150
18. Martínez-Huitle, C.A.; Panizza, M. Electrochemical Oxidation of Organic Pollutants for Wastewater Treatment. *Curr. Opin. Electrochem.* **2018**, *11*, 62–71. https://doi.org/10.1016/j.coelec.2018.07.010.
19. Martínez-Huitle, C.A.; Sirés, I.; Rodrigo, M.A. Editorial Overview: Electrochemical Technologies for Wastewater Treatment with a Bright Future in the Forthcoming Years to Benefit of Our Society. *Curr. Opin. Electrochem.* **2021**, *30*, 100905. https://doi.org/10.1016/J.COELEC.2021.100905.
20. Câmara Cardozo, J.; Barbosa Segundo, I.D.; Galvão, E.R.V.P.; da Silva, D.R.; dos Santos, E.V.; Martínez-Huitle, C.A. Decentralized Environmental Applications of a Smartphone-based Method for Chemical Oxygen Demand and Color Analysis. *Sci. Rep*. **2023**, *13*, 11082. https://doi.org/10.1038/s41598-023-37126-9.
21. Vieira, G.d.F.; Barbosa Segundo, I.D.; Santos, J.E.L.; Gondim, A.D.; dos Santos, E.V.; Martínez-Huitle, C.A. Electro-Oxidation of Wastewater from a Beauty Salon: The Influence of Electrolyte Type in the Removal of Organic Load and Energy Consumption. *Process Saf. Environ. Prot.* **2023**, *177*, 1260–1271. https://doi.org/10.1016/J.PSEP.2023.07.078.
22. Panizza, M.; Cerisola, G. Direct And Mediated Anodic Oxidation of Organic Pollutants. *Chem. Rev.* **2009**, *109*, 6541–6569. https://doi.org/10.1021/cr9001319.
23. Sirés, I.; Brillas, E.; Oturan, M.A.; Rodrigo, M.A.; Panizza, M. Electrochemical Advanced Oxidation Processes: Today and Tomorrow. A Review. *Environ. Sci. Pollut. Res.* **2014**, *21*, 8336–8367. https://doi.org/10.1007/s11356-014-2783-1.
24. Chaplin, B.P. Critical Review of Electrochemical Advanced Oxidation Processes for Water Treatment Applications. *Environ. Sci. Process. Impacts* **2014**, *16*, 1182–1203. https://doi.org/10.1039/C3EM00679D.
25. Zanta, C.L.P.S.; Martínez-Huitle, C.A. Degradation of 2-Hydroxybenzoic Acid by Advanced Oxidation Processes. *Braz. J. Chem. Eng.* **2009**, *26*, 503–513. https://doi.org/10.1590/S0104-66322009000300006.
26. Martínez-Huitle, C.A.; Ferro, S. Electrochemical Oxidation of Organic Pollutants for the Wastewater Treatment: Direct and Indirect Processes. *Chem. Soc. Rev.* **2006**, *35*, 1324–1340. https://doi.org/10.1039/B517632H.
27. Comninellis, C. Electrocatalysis in the Electrochemical Conversion/Combustion of Organic Pollutants for Waste Water Treatment. *Electrochim. Acta* **1994**, *39*, 1857–1862. https://doi.org/10.1016/0013-4686(94)85175-1.
28. Martínez-Huitle, C.A.; Rodrigo, M.A.; Sirés, I.; Scialdone, O.; Martinez-Huitle, C.A.; Rodrigo, M.A.; Sire, I.; Scialdone, O. Single and Coupled Electrochemical Processes and Reactors for the Abatement of Organic Water Pollutants: A Critical Review. *Chem. Rev.* **2015**, *115*, 13362–13407. https://doi.org/10.1021/acs.chemrev.5b00361.
29. Martínez-Huitle, C.A.; Quiroz, M.A.; Comninellis, C.; Ferro, S.; De Battisti, A. Electrochemical Incineration of Chloranilic Acid Using Ti/IrO_2, Pb/PbO_2 and Si/BDD Electrodes. *Electrochim. Acta* **2004**, *50*, 949–956. https://doi.org/10.1016/j.electacta.2004.07.035.

30. Medeiros, M.C.; de Medeiros, J.B.; Martínez-Huitle, C.A.; Oliveira, T.M.B.F.; Mazzetto, S.E.; da Silva, F.F.M.; Castro, S.S.L. Long-Chain Phenols Oxidation Using a Flow Electrochemical Reactor Assembled with a TiO_2-RuO_2-IrO_2 DSA Electrode. *Sep. Purif. Technol.* **2021**, *264*, 118425. https://doi.org/10.1016/j.seppur.2021.118425.
31. Bensalah, N.; Faouzi Ahmadi, M.; Martinez-Huitle, C.A. Electrochemical Oxidation of 2-Chloroaniline in Single and Divided Electrochemical Flow Cells Using Boron Doped Diamond Anodes. *Sep. Purif. Technol.* **2021**, *263*, 118399. https://doi.org/10.1016/j.seppur.2021.118399.
32. Ferreira, M.B.; Rocha, J.H.B.; da Silva, D.R.; de Moura, D.C.; de Araújo, D.M.; Martinez-Huitle, C.A. Application of Electrochemical Oxidation Process to the Degradation of the Novacron Blue Dye Using Single and Dual Flow Cells. *J. Solid State Electrochem.* **2016**, *20*, 2589–2597. https://doi.org/10.1007/s10008-016-3155-1.
33. Brito, L.R.D.; Ganiyu, S.O.; dos Santos, E.V.; Oturan, M.A.; Martínez-Huitle, C.A. Removal of Antibiotic Rifampicin from Aqueous Media by Advanced Electrochemical Oxidation: Role of Electrode Materials, Electrolytes and Real Water Matrices. *Electrochim. Acta* **2021**, *396*, 139254. https://doi.org/10.1016/J.ELECTACTA.2021.139254.
34. Oliveira, E.M.S.; Silva, F.R.; Morais, C.C.O.; Oliveira, T.M.B.F.; Martínez-Huitle, C.A.; Motheo, A.J.; Albuquerque, C.C.; Castro, S.S.L. Performance of (in)Active Anodic Materials for the Electrooxidation of Phenolic Wastewaters from Cashew-Nut Processing Industry. *Chemosphere* **2018**, *201*, 740–748. https://doi.org/10.1016/j.chemosphere.2018.02.037.
35. Panizza, M.; Martinez-Huitle, C.A. Role of Electrode Materials for the Anodic Oxidation of a Real Landfill Leachate—Comparison between Ti-Ru-Sn Ternary Oxide, PbO_2 and Boron-Doped Diamond Anode. *Chemosphere* **2013**, *90*, 1455–1460. https://doi.org/10.1016/j.chemosphere.2012.09.006.
36. Ding, J.; Bu, L.; Zhao, Q.; Kabutey, F.T.; Wei, L.; Dionysiou, D.D. Electrochemical Activation of Persulfate on BDD and DSA Anodes: Electrolyte Influence, Kinetics and Mechanisms in the Degradation of Bisphenol A. *J. Hazard. Mater.* **2020**, *388*, 121789. https://doi.org/10.1016/J.JHAZMAT.2019.121789.
37. Santos, J.E.L.; Antonio Quiroz, M.; Cerro-Lopez, M.; De Moura, D.C.; Martínez-Huitle, C.A. Evidence for the Electrochemical Production of Persulfate at TiO_2 Nanotubes Decorated with PbO_2. *New J. Chem.* **2018**, *42*, 5523–5531. https://doi.org/10.1039/c7nj02604h.
38. Araujo, K.C.; Silva, K.N.; Silva, D.R.D.; Quiroz, M.A.; Martinez-Huitle, C.A.; Santos, E.V. The Green Use of Persulfate Electrochemically Generated with Diamond Electrodes for Depolluting Soils. In *Electrochemical Society Meeting Abstracts 240*; The Electrochemical Society, Inc.: Bristol, UK, 2021; p. 1530.
39. de Freitas Araújo, K.C.; da Silva, D.R.; dos Santos, E.V.; Varela, H.; Martínez-Huitle, C.A. Investigation of Persulfate Production on BDD Anode by Understanding the Impact of Water Concentration. *J. Electroanal. Chem.* **2020**, *860*, 113927. https://doi.org/10.1016/j.jelechem.2020.113927.
40. Araújo, K.C.d.F.; Barreto, J.P.d.P.; Cardozo, J.C.; dos Santos, E.V.; de Araújo, D.M.; Martínez-Huitle, C.A. Sulfate Pollution: Evidence for Electrochemical Production of Persulfate by Oxidizing Sulfate Released by the Surfactant Sodium Dodecyl Sulfate. *Environ. Chem. Lett.* **2018**, *16*, 647–652. https://doi.org/10.1007/s10311-017-0703-6.
41. Gurung, K.; Ncibi, M.C.; Shestakova, M.; Sillanpää, M. Removal of Carbamazepine from MBR Effluent by Electrochemical Oxidation (EO) Using a Ti/Ta_2O_5-SnO_2 Electrode. *Appl. Catal. B* **2018**, *221*, 329–338. https://doi.org/10.1016/j.apcatb.2017.09.017.
42. Dai, Q.; Zhou, J.; Meng, X.; Feng, D.; Wu, C.; Chen, J. Electrochemical Oxidation of Cinnamic Acid with Mo Modified PbO_2 Electrode: Electrode Characterization, Kinetics and Degradation Pathway. *Chem. Eng. J.* **2016**, *289*, 239–246. https://doi.org/10.1016/j.cej.2015.12.054.
43. Espinoza-Montero, P.J.; Martínez-Huitle, C.A.; Loor-Urgilés, L.D. Technologies Employed for Carwash Wastewater Recovery. *J. Clean. Prod.* **2023**, *401*, 136722. https://doi.org/10.1016/J.JCLEPRO.2023.136722.
44. Yao, Y.; Teng, G.; Yang, Y.; Huang, C.; Liu, B.; Guo, L. Electrochemical Oxidation of Acetamiprid Using Yb-Doped PbO_2 Electrodes: Electrode Characterization, Influencing Factors and Degradation Pathways. *Sep. Purif. Technol.* **2019**, *211*, 456–466. https://doi.org/10.1016/J.SEPPUR.2018.10.021.
45. Carvalho De Almeida, C.; Ganiyu, S.O.; Martínez-Huitle, C.A.; Vieira, E.; Santos, D.; Barrios Eguiluz, K.I.; Salazar-Banda, G.R.; Ganiyu, S.O. Unprecedented Formation of Reactive BrO–Ions and Their Role as Mediators for Organic Compounds Degradation: The Fate of Bromide Ions Released during the Anodic Oxidation of Bromophenol Blue Dye. *Electrochem. Sci. Adv.* **2022**, *1*, e2100225. https://doi.org/10.1002/ELSA.202100225.
46. Oliveira, H.L.; Barros, T.M.; Santos, J.E.L.; Gondim, A.D.; Quiroz, M.A.; Martínez-Huitle, C.A.; dos Santos, E.V. Electrochemical Oxidation of a Real Effluent Using Selective Cathodic and Anodic Strategies to Simultaneously Produce High Value-Added Compounds: Green Hydrogen and Carboxylic Acids. *Electrochem. Commun.* **2023**, *154*, 107553. https://doi.org/10.1016/J.ELECOM.2023.107553.
47. Ganiyu, S.O.; Martínez-Huitle, C.A. The Use of Renewable Energies Driving Electrochemical Technologies for Environmental Applications. *Curr. Opin. Electrochem.* **2020**, *22*, 211–220. https://doi.org/10.1016/j.coelec.2020.07.007.